Available online at www.elixirpublishers.com (Elixir International Journal)

Computational Chemistry

Elixir Comp. Chem. 93 (2016) 39522-39528

ISSN: 2229-712X

Vibrational Analysis First Hyperpolarizability and Homo-Lumo Analyses of 2, 4, 6-Trimethyl Benzaldehyde

G.Vijayakumar* and N.Saravanan

Department of Chemistry A.A. Government Arts College, Musiri- 621 211, Tamil Nadu, India.

ARTICLE INFO

Article history:

Received: 31 March 2016;

Received in revised form:

3 April 2016;

Accepted: 9 April 2016;

Keywords

FT-IR,

FT-Raman spectra,

HOMO–LUMO energy.

ABSTRACT

In the present study, the FT-IR and FT-Raman spectra of 2,4,6-Trimethylbenzaldehyde (TMB) have been recorded in the region 4000–400 cm^{-1} and 3500–50 cm^{-1}, respectively. The fundamental modes of vibrational frequencies of TMB are assigned. Theoretical information on the optimized geometry, harmonic vibrational frequencies, infrared and Raman intensities were obtained by means of ab initio Hartree–Fock (HF) and density functional theory (DFT) gradient calculations with complete relaxation in the potential energy surface using 6-31+G(d,p)) basis set. The vibrational frequencies which were determined experimentally from the spectral data are compared with those obtained theoretically from ab initio and DFT calculations. A close agreement was achieved between the observed and calculated frequencies by refinement of the scale factors. The infrared and Raman spectra were also predicted from the calculated intensities. Thermodynamic properties like entropy, heat capacity, zero point energy, have been calculated for the molecule. The calculated HOMO–LUMO energy gap reveals that charge transfer occurs within the molecule. Unambiguous vibrational assignment of all the fundamentals was made using the total energy distribution (TED).

1. Introduction

Modern vibrational spectrometry has proven to be an exceptionally powerful technique for solving many chemistry problems. It has been extensively employed both in the study of chemical kinetics and chemical analysis. For a proper understanding of IR and Raman Spectra, a reliable assignment of all vibrational band is essential. For this purpose, several theoretical methods are useful in analyzing vibrational spectra of organic molecules. Accurate vibrational assignment for aromatic and another conjugated system is necessary for characterization of materials. Quantum chemical computational methods have proven to be an essential tool for interpreting and predicting vibrational spectra [1,2]. A significant advance in this area was made by scaled quantum mechanical (SQM) force field method [3-6]. In the SQM approach the systematic errors of the computed harmonic force field are corrected by a few scale factors which were found to be well transferable between chemically related molecules [7-9].

The vibrational spectra of benzaldehyde and its derivatives have been studied earlier [10-15]. The substitution of a functional group changes the spectra markedly. Recent spectroscopic studies of the benzaldehyde and their derivatives have been motivated because the vibrational spectra are very useful for the understanding of specific biological process and in the analysis of relatively complex systems. The vibrational analysis of 2,4,6-Trimethylbenzaldehyde (TMB) have been carried out by applying the HF/6-31+G(d,p) and B3LYP/6-31+G(d,p) based on SQM method [16-19].

In the framework of DFT approach, various exchange and correlation functionals are routinely used. Among these, Becke-3-Lee-yang-parr (B3LYP) functional is the best in predicting results for molecular geometry and vibrational wave numbers for moderately large molecules [20-22]. Owing to these applications, an attempt has been made in this study to interpret the vibrational spectra of TMB.

In the present investigation, the detailed vibrational spectral analysis of the TMB is performed by combining the experimental and theoretical information using *ab initio* (HF) and density functional theory (B3LYP) to derive information about electronic effects and intramolecular charge transfer responsible for biological activity. By combining all these facts into account, the present study has been aimed, to investigate the vibrational spectra of TMB. Investigations have also been carried out to identify the NLO property (first-hyperpolarizability), HOMO-LUMO energies of the optimized molecular structure. The spectral features were subsequently assigned to the different normal modes of vibration analysis of the FT-IR and FT-Raman spectra. The harmonic frequencies of TMB was calculated by *ab initio* HF and DFT method and reported along with observed fundamental vibrational frequencies.

2. Experimental Details

The fine sample of TMB was purchased from Lancaster chemical company, UK and used as such for the spectral measurements. The Fourier transform infrared spectrum of the title compound is measured in the region 4000-400 cm^{-1} at a resolution of ± 1 cm^{-1} using BRUKER IFS 66V vacuum Fourier transform spectrometer equipped with an MCT detector, a KBr beam splitter and globar arc source. The FT-Raman spectrum was recorded on a computer interfaced BRUKET IFS model interferometer equipped with FRA106 FT-Raman accessory in the 3500-100 cm^{-1} stokes region using the 1064 nm line of a Nd YAG laser for excitation operating at

Tele:

E-mail address: n79saravanan@gmail.com

200 mn power. The reported wave numbers are believed to be accurate within ±1 cm^{-1}.

3. AB Initio and Dft Calculations

Quantum chemical density functional calculations are carried out for TMB with the 2009 Window version of the GAUSSIAN suite program [23] using *ab initio* (HF) and Becke-3-Lee-Yang-Parr (B3LYP) functional [24-27] supplemented with the standard 6-31+G(d,p) basis set. All the parameters were allowed to relax and all the calculations converged to an optimized geometry which corresponds to a true energy minimum, as revealed by the lack of imaginary values in the wave number calculations. The cartesian representation of the theoretical force constants have been computed at the fully optimized geometry by assuming the molecule belongs to C_S point group symmetry. The transformation of force field from cartesian to internal local-symmetry coordinates, the scaling, the subsequent normal coordinate analysis calculation of total energy distribution (TED) are done on a PC with the version V7.0-G77 of the MOLVIB program written by Sundius [28-30].

3.1. Prediction of Raman intensities

The Raman activities (S_i) calculated by the GAUSSIAN-09W program were converted to relative Raman intensities (I_i) using the following relationship [31-34]

$$I_i = \frac{f(\nu_o - \nu_i)^4 S_i}{\nu_i\left[1 - \exp\left(\frac{-hc\nu_i}{kT}\right)\right]} \qquad \text{--------(1)}$$

where ν_o is the exciting frequency (in cm^{-1} units); ν_i is the vibrational wave number of the i^{th} normal mode; h, c and k are the universal constants; and f is the suitably chosen common scaling factor for all the peak intensities. For simulation of Raman spectrum, pure Lorentzian line shapes were used with a bandwidth of 10 cm^{-1}.

4. Results and Discussions

4.1. Molecular geometry

The optimized molecular structure of TMB is shown in Fig. 1. The optimized geometrical parameter of TMB is calculated by *ab initio* (HF) and DFT (B3LYP) levels with the 6-31+G(d,p) basis set are listed in Tables 1.

The global minimum energy obtained by HF & DFT method with 6-31+G(d,p) basis sets are calculated as -460.36548519 Hartrees and -463.42127194 Hartrees respectively.

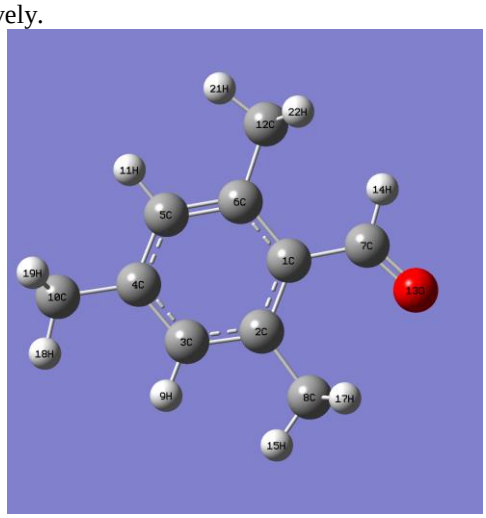

Fig 1. Molecular structure of 2,4,6-Trimethyl benzaldehyde

2. Vibrational Spectra

TMB consists of 23 atoms and its 63 normal modes are distributed amongst the symmetry species as: Γ_{3N-6} = 43A' (in-plane) + 20A" (out-of-plane).

The detailed vibrational assignment of fundamental modes of TMB along with the calculated IR and Raman frequencies and normal mode descriptions (characterised by TED) are reported in Table 2. Also the force constant, IR intensities and Raman activities of TMB is given in Table 2. The FT-IR and FT-Raman spectra of the TMB are shown in figs. 2 and.3, respectively.

C–H Vibrations

Aromatic compounds commonly exhibit multiple weak bands in the region 3100 – 3000 cm^{-1} due to aromatic C–H stretching vibrations [35,36]. The bands due to C–H in-plane bending vibrations interact somewhat with C–C stretching vibrations are observed as a number of bands in the region 1300 – 1000 cm^{-1}. The C–H out-of-plane bending vibrations [37,38] occur in the region 900 – 667 cm^{-1}. In this region the bands are not affected appreciable by the nature of the substituents. In the present investigation, the FT-IR band identified at 3180, 2990 cm^{-1} and 3020 cm^{-1} in the FT-Raman are assigned to C–H stretching vibrations. The C–H in-plane and out-of-plane bending modes are also assigned within the characteristic region and are presented in Table 2.

C–C Vibrations

The bands between 1400 – 1650 cm^{-1} in benzene derivatives are due to C–C stretching vibrations [39]. Therefore, the FT-IR and FT-Raman bands found at 1830, 1730,1690,1650,1440,1420 cm^{-1} and 1680,1580,1480,1430 cm^{-1} have been assigned to C–C stretching vibrations of TMB respectively. Also, the ring modes are affected by the substitutions in the aromatic ring of the title compound. Accordingly, in the present investigation, the FT-IR and FT-Raman bands observed at 1040,980 cm^{-1} and 1020,970 cm^{-1} have been assigned to ring in-plane bending modes of TMB, respectively. The ring out-of-plane bending modes of TMB are also listed in Table 2. The reductions in the frequencies of these modes are due to the change in force constant and the vibrations of functional groups present in the molecule.

C=O Vibrations

The carbonyl bonds are the most characteristic bands of infrared spectrum. Both the carbon and oxygen atoms of the carbonyl group move during vibration and they have nearly equal amplitudes. The carbonyl frequencies can be altered by intermolecular hydrogen bonding. A great deal of structural information can be derived from the exact position of the carbonyl stretching absorption peaks. Normally carbonyl group vibrations [40] occur in the region 1800 – 1700 cm^{-1}. Accordingly in the present investigation the FT-IR band appearing at 2210 cm^{-1} is assigned as C=O stretching vibration. The C=O in-plane bending and out-of-plane bending vibration are also identified for TMB and also listed in Table 2.

CH_3 Vibrations

For the assignments of CH_3 group frequencies, nine fundamental vibrations can be associated to each CH_3 group. Three stretching, three bending, two rocking modes and single torsion mode describe the motion of the methyl group. In aromatic compounds, the CH_3 asymmetric stretching vibrations are expected in the range 2925 – 3000 cm^{-1} and the symmetric CH_3 vibrations [41] in the range 2905 – 2940 cm^{-1}.

Table 1. Optimized geometrical parameters of 2,4,6-trimethyl benzaldehyde obtained by HF/6-31+G(d,p) and B3LYP/6-31+G(d,p) basis set calculations.

Bond Length	Value (Å)		Bond Angle	Value (°)		Dihedral Angle	Value (°)	
	6-31+G(d,p)			6-31+G(d,p)			6-31+G(d,p)	
	HF	B3LYP		HF	B3LYP		HF	B3LYP
C1-C2	1.4082	1.427	C2-C1-C6	119.7187	119.7942	C6-C1-C2-C3	0.0864	0.0
C1-C6	1.4123	1.4269	C2-C1-C7	121.8839	121.8609	C6-C1-C2-C8	-179.7881	179.9996
C1-C7	1.47	1.4689	C6-C1-C7	118.3973	118.3449	C7-C1-C2-C3	179.9789	-180.0
C2-C3	1.3935	1.4021	C1-C2-C3	118.7074	118.7511	C7-C1-C2-C8	0.1044	-0.0003
C2-C8	1.5113	1.512	C1-C2-C8	122.8658	123.1726	C2-C1-C6-C5	-0.1013	0.0002
C3-C4	1.387	1.4026	C3-C2-C8	118.4267	118.0763	C2-C1-C6-C12	179.744	-179.9994
C3-H9	1.0737	1.087	C2-C3-C4	122.2384	122.0509	C7-C1-C6-C5	-179.9975	180.0001
C4-C5	1.3931	1.4042	C2-C3-H9	118.5766	118.7022	C7-C1-C6-C12	-0.1522	0.0005
C4-C10	1.5086	1.5116	C4-C3-H9	119.185	119.2469	C2-C1-C7-O13	0.1201	0.0047
C5-C6	1.3856	1.3994	C3-C4-C5	118.308	118.4876	C2-C1-C7-H14	-179.9287	180.0048
C5-H11	1.0745	1.0871	C3-C4-C10	120.8492	121.2133	C6-C1-C7-H13	-179.9861	-179.9953
C6-C12	1.5171	1.5196	C5-C4-C10	120.8343	120.2992	C6-C1-C7-H14	-0.0349	0.0049
C7-O13	1.2231	1.2506	C4-C5-C6	121.8363	121.5632	C1-C2-C3-C4	0.1597	-0.0006
C7-H14	1.0808	1.0997	C4-C5-H11	119.1728	119.2224	C1-C2-C3-H9	-179.7813	179.9991
C8-H15	1.0822	1.0948	C6-C5-H11	118.9908	119.2143	C8-C2-C3-C4	-179.9601	179.9997
C8-H16	1.0815	1.0951	C1-C6-C5	119.19	119.353	C8-C2-C3-H9	0.0989	-0.0005
C8-H17	1.0815	1.0951	C1-C6-C12	122.6561	122.587	C1-C2-C8-H15	179.8916	179.9961
C10-H18	1.0821	1.0953	C5-C6-C12	118.1538	118.0599	C1-C2-C8-H16	-59.0508	-59.3479
C10-H19	1.0847	1.0952	C1-C7-O13	126.3129	126.0901	C1-C2-C8-H17	58.8134	59.3408
C10-H20	1.0847	1.099	C1-C7-H14	115.7958	116.1492	C3-C2-C8-H15	0.0168	-0.0042
C12-H21	1.0814	1.0941	O13-C7-H14	117.8912	117.7607	C3-C2-C8-H16	121.0743	120.6517
C12-H22	1.084	1.0966	C2-C8-H15	110.0231	109.7577	C3-C2-C8-H17	-121.0614	-120.6596
C12-H23	1.084	1.0966	C2-C8-H16	111.7341	111.5574	C2-C3-C4-C5	-0.3816	0.001
			C2-C8-H17	111.754	111.5569	C2-C3-C4-C10	178.5734	-179.9949
			H15-C8-H16	108.8728	108.7894	H9-C3-C4-C5	179.5591	-179.9987
			H15-C8-H17	108.8786	108.7892	H9-C3-C4-C10	-1.4859	0.0054
			H16-C8-H17	105.426	106.2744	C3-C4-C5-C6	0.3648	-0.0009
			C4-C10-H18	111.437	111.3309	C3-C4-C5-H11	-179.5645	179.9987
			C4-C10-H19	111.4663	110.9112	C10-C4-C5-C6	-178.5904	179.9951
			C4-C10-H20	110.8475	110.9137	C10-C4-C5-H11	1.4803	-0.0053
			H18-C10-H19	108.21	107.9851	C3-C4-C10-H18	32.1558	-0.1334
			H18-C10-H20	107.2987	107.9873	C3-C4-C10-H19	153.1633	120.1353
			H19-C10-H20	107.3889	107.5612	C3-C4-C10-H20	-87.2739	-120.4066
			C6-C12-H21	109.882	109.8703	C5-C4-C10-H18	-148.9156	179.8707
			C6-C12-H22	112.3002	112.0451	C5-C4-C10-H19	-27.9082	-59.8606
			C6-C12-H23	112.3007	112.0455	C5-C4-C10-H20	91.6546	59.5975
			H21-C12-H22	107.3587	107.4022	C4-C5-C6-C1	-0.1287	0.0003
			H21-C12-H23	107.3532	107.4017	C4-C5-C6-C12	-179.981	-180.0001
			H22-C12-H23	107.396	107.8563	H11-C5-C6-C1	179.8006	-179.9993
						H11-C5-C6-C12	-0.0516	0.0003
						C1-C6-C12-H21	-179.9439	-180.0029
						C1-C6-C12-H22	-60.5223	-60.6988
						C1-C6-C12-H23	60.6411	60.6934
						C5-C6-C12-H21	-0.0971	-0.0025
						C5-C6-C12-H22	119.3245	119.3016
						C5-C6-C12-H23	-119.5121	-119.3061

For numbering of atoms refer Fig. 1.

Table 2. The observed (FT-IR and FT-Raman) and calculated (Unscaled and Scaled) frequencies (cm^{-1}), IR intensity (Km mol^{-1}), Raman Activity ($Å^4$ amu^{-1}) and probable assignments (characterized by TED) of 2,4,6-Trimethylbenzaldehyde using HF/6-31+G(d,p) and B3LYP/6-31+G(d,p) basis set calculations.

S. No	Symmetry Species C_S	Observed fundamentals (cm^{-1})		Calculated values								TED(%) among types of internal coordinates
				HF/6-31+G(d,p)				B3LYP/6-31+G(d,p)				
		FT-IR	FT-Raman	Unscaled frequencies (cm^{-1})	Scaled frequencies (cm^{-1})	IR intensity	Raman activity	Unscaled frequencies (cm^{-1})	Scaled frequencies (cm^{-1})	IR intensity	Raman activity	
1	A′	3180	-	3358	3190	20.1675	101.0348	3287	3184	16.4041	140.5727	γCH(99)
2	A′	-	3020	3348	3028	26.2502	86.4109	3183	3023	32.8132	75.3296	γCH(98)
3	A′	2990	-	3285	3000	10.3967	60.1634	3127	2994	20.4271	59.7265	γCH(98)
4	A′	-	2940	3281	2952	10.9705	73.7146	3126	2946	20.3238	80.0365	γCH_3ips (85)+ γCH(15)
5	A′	2930	-	3280	2938	27.5487	58.8769	3126	2933	15.0541	49.2868	γCH_3ips (84)+γCH(16)
6	A′	2890	-	3273	2900	22.2004	64.3894	3119	2894	8.0731	65.3093	γCH_3ips (82)+γCH (18)
7	A′	-	2880	3266	2890	73.0736	82.7158	3102	2886	14.5838	71.2968	γCH_3ss(82)
8	A′	2790	-	3254	2797	18.8770	69.4232	3097	2793	20.5264	97.1523	γCH_3ss(82)
9	A′	-	2780	3246	2790	18.7496	91.8765	3052	2783	20.4730	209.2531	γCH_3ss(82)
10	A′	2670	-	3210	2680	29.5369	147.6802	3046	2676	60.5598	235.6932	γCH_3ops (84)
11	A′	2600	-	3195	2609	20.4862	145.8812	3035	2602	27.3146	296.8273	γCH_3ops (84)
12	A′	-	2590	3190	2597	33.2604	210.9287	3025	2592	59.1498	42.7102	γCH_3ops (84)
13	A′	2210	-	1844	2222	314.9387	117.2692	1662	2213	40.5863	12.0584	γC=0 (80)+ CH_3ops(20)
14	A′	2100	-	1798	2110	161.8196	122.9773	1649	2102	299.2825	212.6216	γCH_3ipb(79)H_γC=0(21)
15	A′	2000	-	1744	2012	71.2125	35.9677	1596	2006	88.3526	53.5395	γCH_3ipb(79)+CH_3ops(21)
16	A′	1940	-	1666	1949	3.5620	25.9819	1544	1941	4.6328	21.2861	γCH_3ipb(78)+γCC(22)
17	A′	1830	-	1654	1837	10.0579	15.5232	1536	1832	11.0868	13.4240	γCC(80)
18	A′	1730	-	1648	1736	29.8037	10.6498	1528	1731	22.9534	11.6013	γCC(80)
19	A′	1690	-	1647	1699	3.6725	3.1159	1528	1691	20.8527	14.2863	γCC(78)
20	A′	-	1680	1642	1688	12.0267	15.3341	1523	1682	4.1879	13.8827	γCC(79)
21	A′	1650	-	1638	1659	7.5182	11.6179	1513	1651	10.1717	10.1186	γCC(78)+CH_3sb(22)
22	A′	-	1620	1616	1628	16.3054	6.4480	1492	1622	18.7736	2.7593	γCH_3sb(80)+γCC(20)
23	A′	1610	-	1591	1621	8.0295	3.0858	1473	1613	3.3710	5.1805	γCH_3sb(80)+γCC(20)
24	A′	-	1580	1586	1587	29.2650	12.5889	1466	1582	50.6564	27.3098	γCC(79)+CH_3sb(21)
25	A′	1570	-	1581	1577	4.5524	8.4514	1460	1573	1.4673	25.6511	γCH_3sb(80)+γCC(20)
26	A′	-	1480	1578	1489	8.3230	17.0782	1455	1483	4.2672	26.4307	γCC(79)+CH_3sb(21)
27	A′	1440	-	1568	1452	21.4433	1.8939	1447	1444	28.0904	4.6488	γCC(79)+CH_3sb(21)
28	A′	-	1430	1430	1438	4.1444	12.4438	1352	1431	9.4423	9.4955	γCC(79)
29	A′	1420	-	1417	1431	19.5992	7.0038	1328	1425	5.6544	39.8853	γCC(78)+bCH(22)
30	A′	1380	-	1365	1389	24.0375	20.0512	1308	1382	20.0346	7.2552	bCH(84)+ γCC(16)
31	A′	-	1370	1340	1377	15.8526	12.0600	1256	1374	28.6970	13.5835	bCH(80)
32	A′	1350	-	1272	1359	28.4214	26.5501	1191	1351	24.1410	21.4031	bCH(79)
33	A′	-	-	1214	1317	17.3735	0.3953	1096	1333	17.1310	0.1310	Rsymd(75)+bCH(25)
34	A′	-	1300	1201	1313	0.0026	0.3705	1095	1302	0.1533	0.1158	Rsymd(74)+bC=0(26)
35	A′	-	1260	1199	1267	0.0031	1.0435	1094	1262	3.5057	0.3120	bC=0(79)
36	A′	1250	-	1167	1257	2.1036	0.6241	1092	1251	0.8635	0.0924	CH_3ipr (75)+bC=0(25)
37	A′	-	1220	1146	1229	1.2811	2.3509	1060	1223	0.0055	2.4419	CH_3ipr (75)+bC=0(25)
38	A′	-	1160	1139	1169	4.2671	2.9090	1057	1164	0.4797	1.8768	CH_3ipr (74)+Rtrigd(26)
39	A′	1140	-	1131	1149	1.0604	2.7489	1022	1141	2.6524	1.2817	Rtrigd(75)
40	A′	1040	-	1061	1052	0.6259	14.1842	995	1044	1.9405	12.6222	bC-C(76)
41	A′	-	1020	1039	1031	0.0439	0.0599	969	1021	2.3393	0.2836	bC-C(76)+Rtrigtd(24)
42	A′	980	-	1034	994	3.8917	1.2004	924	986	0.0662	0.1318	bC-C(75)+ωCH(25)
43	A′	-	970	1002	981	34.4320	0.1144	892	972	22.6860	0.0420	bC-C(74)+ ωCH(26)
44	A″	960	-	855	969	53.2387	6.0427	798	962	33.4746	8.1853	CH_3opb(80)+ ωCH(20)
45	A″	940	-	832	951	4.5959	0.2332	740	943	3.3008	0.2542	CH_3opb(80)+ ωCH(20)
46	A″	880	-	676	893	7.0396	3.0753	633	874	5.2330	4.1238	CH_3opb(79)+ ωCH(20)
47	A″	840	-	644	852	3.8857	1.0222	579	842	0.9680	15.8306	ωCH(80)+bcc(20)
48	A″	-	790	612	801	0.1300	0.6092	573	794	1.3633	11.6580	ωCH(80)
49	A″	780	-	611	793	0.0026	31.6033	552	785	0.0287	0.3489	ωCH(79)+tRsymd (21)
50	A″	-	720	582	733	2.6984	5.5246	544	726	1.5391	5.2268	tRsymd(82)
51	A″	710	-	531	718	9.4657	0.3462	492	711	7.6755	0.4541	ωC=0(75)+CH_3opr(25)
52	A″	630	-	418	641	0.7068	5.8012	392	633	0.4839	7.1657	CH_3opr (80)+ ωC=0(20)
53	A″	-	620	365	630	3.8819	1.6430	332	622	2.4920	0.8515	CH_3opr(81)
54	A″	-	580	352	587	2.2097	0.7976	329	582	1.8400	1.2744	CH_3opr (80)
55	A″	560	-	318	569	2.0304	0.5967	298	563	1.6472	0.4414	tRasymd(72)
56	A″	540	-	260	547	8.0262	0.9802	242	543	5.6304	1.3302	ωCC(74)+tRasymd(26)
57	A″	-	530	255	537	0.5476	1.9673	235	531	0.7592	2.2258	ωCC(74)
58	A″	490	-	231	495	0.0004	0.0953	205	492	0.2914	0.1293	ωCC(74)
59	A″	-	480	224	487	2.6666	0.3780	199	483	2.8484	0.4209	ωCC(71)+tRasymd(29)
60	A″	-	400	191	406	6.1955	0.1726	174	402	4.8740	0.1772	tRtrigd(65
61	A″	-	310	126	319	5.6920	1.2540	126	313	4.3912	1.8087	CH_3twist(50)
62	A″	-	230	71	238	8.8702	0.4024	74	236	3.5199	0.1366	CH_3twist(50)
63	A″	-	210	13	217	0.1086	0.2976	36	211	0.2323	0.8452	CH_3twist(50)

For CH_3 symmetric stretching frequency is established at 2890cm^{-1} in FT-IR and 2880, 2780 cm^{-1} in FT-Raman. CH_3 asymmetry in-plane stretch frequencies are assigned at 2930, 2870 cm^{-1} in FTIR and in FT –Raman peaks are observed at 2940 cm^{-1} for the title compound. These assignments are also supported by the literature [40]. The two in-plane hydrogen deformation modes are also well established. The symmetrical methyl deformation mode is observed at 1650,1570 cm^{-1} and 1620 cm^{-1} in the FT-IR and FT-Raman spectrum respectively. The band at 2670, 2600cm^{-1} in FT-IR and 2590 cm^{-1} in FT-Raman is attributed to CH_3 out of plane stretching and the FT-IR peaks observed at 960, 940, 880 cm^{-1} out-of-plane bending modes in the all species. The methyl deformation modes mainly couple with in-plane bending vibrations. The bands obtained at 1250 cm^{-1} in FT-IR and 1220,1160 cm^{-1} in FT-Raman is measured in CH_3 in-plane and out-of-plane rocking modes respectively. The assignment of the band at 310,230,210 cm^{-1} in FT-Raman is attributed to methyl twisting mode.

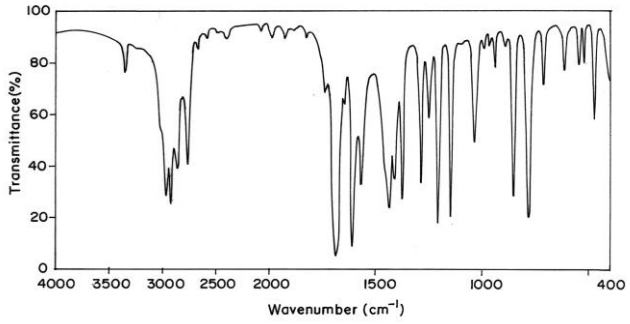

Fig 2. FTIR spectrum of 2,4,6-Trimethyl benzaldehyde

5. Homo–Lumo Analysis

The interaction of two atomic (or) molecular orbital's produces two new orbital. One of the new orbital's is higher in energy than the original ones (the anti bonding orbital) and one is lower (the bonding orbital). When one of the initial orbital's is filled with a pair of electrons (a Lewis base) and the other is empty (a Lewis acid), we can place the two electrons into the lower, energy of the two new orbital's. The "filled-empty" interaction therefore is stabilizing. When we are dealing with interacting molecular orbital's, the two that interact are generally the highest energy occupied molecular orbital (LUMO) of the molecule. These orbital's are the pair of orbitals in the molecule, which allows them to interact most strongly. These orbital's are sometimes called the frontier orbital's, because they lie at the outermost boundaries of the electrons of molecule. The HOMO-LUMO analysis for the title molecule has been carried out using B3LYP/6-31+G (d,p) level.

By contrast, the HOMO is located over methyl group whereas LUMO is located on ring and methyl group atoms of 2,4,6-Trimethyl benzaldehyde. The atomic orbital compositions of the frontier molecular orbital are shown in Fig.4. The HOMO → LUMO energy gap of 2, 4, 6-Trimethyl benzaldehyde obtained by B3LYP/6-31+G (d,p) density functional calculations, reveals that the energy gap reflects the chemical activity of the molecules. The LUMO as an electron acceptor (EA) represents the ability to obtain an electron (ED), and HOMO represents the ability to donate an electron(ED). The ED groups to the efficient EA groups through π-conjugated path.

E_{HOMO} = –0.33282 a.u.

E_{LUMO} = 0.06400 a.u.

Energy gap = 0.39682 a.u.

The energy gap explains the fact that eventual charge transfer interaction is taking place within the molecule.

6. Non-Linear Optical Effects

Polarizabilities and hyperpolarizabilities characterize the response of a system in an applied electric field [42]. They determine not only the strength of molecular interactions (long-range intermolecular induction, dispersion forces, etc.) as well as the cross sections of different scattering and collision processes, but also the non-linear optical properties (NLO) of the system [43,44]. It has been found that the dye sensitizer hemicyanine system, which has high NLO property, usually possesses high photoelectric conversion performance [45]. The polarizabilities and hyperpolarizabilities are used to investigate the relationships among photocurrent generation, molecular structures and NLO [46].

The first hyperpolarizability (β) of the molecular system, and related properties (α_0 and Δα) of TMB are calculated using B3LYP/6-31+G(d,p) basis set, based on the finite-field approach. In the presence of an applied electric field, the energy of a system is a function of the electric field. First hyperpolarizability is a third rank tensor that can be described by a 3 × 3 × 3 matrix. The 27 components of the 3D matrix can be reduced to 10 components due to the Kleinman symmetry [47]. It can be given in the lower tetrahedral format. It is obvious that the lower part of the 3 × 3 × 3 matrix is a tetrahedral. The components of β are defined as the coefficients in the Taylor series expansion of the energy in the external electric field. When the external electric field is weak and homogeneous, this expansion becomes:

$$E = E^0 - \mu_\alpha F_\alpha - \frac{1}{2}\alpha_{\alpha\beta}F_\alpha F_\beta - \frac{1}{6}\beta_{\alpha\beta\gamma}F_\alpha F_\beta F_\gamma + \ldots \quad \ldots (1)$$

Where E^0 is the energy of the unperturbed molecules, F_α, the field at the origin and μ_α, $\alpha_{\alpha\beta}$ and $\beta_{\alpha\beta\gamma}$ are the components of dipole moment, polarizability and the hyperpolarizability, respectively. The total static dipole moment μ, the mean polarizability α_0, the anisotropy of the polarizability Δα and the mean first hyperpolarizability β, using the X, Y, Z components they are defined as follows:

$\mu = (\mu^2_x+\mu^2_y+\mu^2_z)^{1/2}$

$\alpha_0 = (\alpha_{xx}+\alpha_{yy}+\alpha_{zz})/3$

$\beta = (\beta^2_x+\beta^2_y+\beta^2_z)^{1/2}$

and

$\beta_x = \beta_{xxx} + \beta_{xyy} + \beta_{xzz}$

$\beta_y = \beta_{yyy} + \beta_{xxy} + \beta_{yzz}$

$\beta_z = \beta_{zzz} + \beta_{xxz} + \beta_{yyz}$

Since the standard values of the polarizability α and first hyperpolarizability β are reported in atomic units (a.u.), the calculated values should have been converted into electrostatic units (esu). (α: 1 a.u. = 0.1482 × 10^{-24} e.s.u; β: 1 a.u. = 8.6393 × 10^{-33} e.s.u).

The calculated polarizability (α_0), the first hyperpolarizability (β) and its component values of the title compound are listed in Table 4.3.The calculated total static dipole moment (μ), mean polarizability (α_0) and hyperpolarizability (β) are 1.45534 Debye, 13.6969 × 10^{-24} e.s.u and 6.7438 × 10^{-30} e.s.u by DFT method.

7. Thermodynamic Properties

The thermodynamic parameters such as total thermal energy, heat capacity at constant volume, entropy, vibrational energy, zero point vibrational energy and rotational constants

are calculated employing HF/6-31+G(d,p) and B3LYP/6-31+G(d,p) methods and they are presented in Table 4. Dipole moment reflects the molecular charge distribution and is given as a vector in three dimensions. Therefore, it can be used as descriptor to depict the charge movement across the molecule. Direction of the dipole moment vector in a molecule depends on the centers of positive and negative charges. Dipole moments are strictly determined for neutral molecules. For charged systems, its value depends on the choice of origin and molecular orientation.

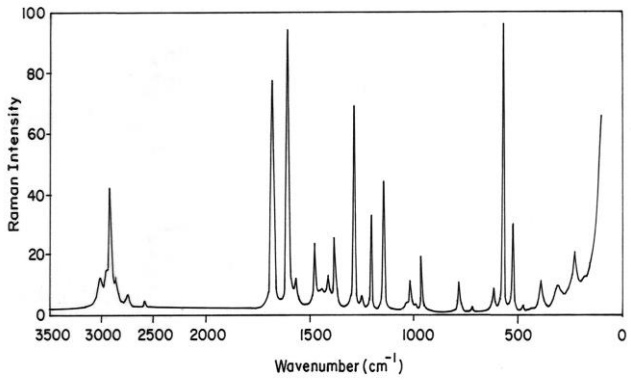

Fig 3. FT-Raman spectrum of 2,4,6-Trimethyl benzaldehyde

Table 3. The calculated first hyperpolarizabilities of 2,4,6-trimethylbenzaldehyde using B3LYP/6-31+G(d,p) method.

Parameters	2,4,6-trimethyl benzaldehyde
	B3LYP/6-31+G(d,p)
β_{xxx}	52.3182548
β_{xxy}	–44.6951421
β_{xyy}	–325.1116452
β_{yyy}	–309.23064
β_{xxz}	-274.1652629
β_{yyz}	–5.4890705
β_{xzz}	–17.6140545
β_{yzz}	7.4062789
β_{zzz}	29.2649763
β	3.5978×10^{-30} esu
Dipole moment	4.1471 Debye

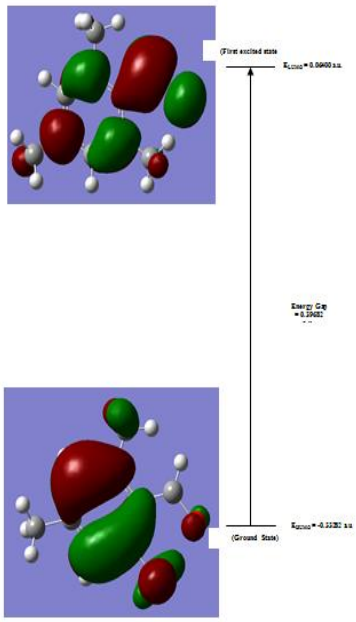

Fig 4. The atomic orbital HOMO-LUMO composition of frontier molecular orbital for 2,4,6-Trimethyl benzaldehyde

Table 4. Thermodynamic properties of 2,4,6-trimethylbenzaldehyde.

Parameters	2,4,6-trimethyl benzaldehyde	
	HF	B3LYP
	6-31+G(d,p)	6-31+G(d,p)
Zero point vibrational energy (Kcal/Mol)	130.54109	122.00861
Rotational constants (GHZ)		
A	1.67255	1.64722
B	0.92337	0.90952
C	0.60144	0.59241
Entropy (Cal/Mol-Kelvin)	103.480	98.326
Specific heat capacity at constant volume (Cal/Mol-Kelvin)	38.448	39.199
Total (Thermal) energy(KCal/Mol)	137.194	128.487
Translational energy(KCal/Mol)	0.889	0.889
Rotational energy(KCal/Mol)	0.889	0.889
Vibrational energy(KCal/Mol)	135.417	126.710
Dipole moment	4.2409	4.1471

Conclusion

DFT and ab initio calculations have been carried out on the structure and vibrational spectra of 2,4,6-Trimethyl benzaldehyde. Comparison between the calculated and experimental structural parameters indicates that B3LYP results are in good agreement with experimental values. Vibrational frequencies calculated by HF/6-31+G(d,p) and B3LYP/6-31+G(d,p) method agree well with experimental results. The assignments made at higher level of theory with higher basis set with only reasonable deviations from the experimental values, seem to be correct. The various properties of TMB are discussed by studying non-linear optical effects and its thermodynamic properties.

References

[1] Pulay P, Zhou X, Fogarasi G, in: R. Fransto (Ed.), NATO ASI series, Vol. C, 406, Kluwer, Dordrecht, 1933, P.99

[2] Hess Jr. B A, Schaad J, Carsky P, Zahradnik R, Chem. Rev., 86 (1986) 709.

[3] Pulay P, Fogarasi G, Pongor G, Boggs J E, Vargha A, J. Am. Chem. Soc. 105 (1983) 7037.

[4] Fogarasi G, Pulay P, in : J.R. Durig (Ed.), Vibrational Spectra and Structure, Vol.14, Elsevier, Amsterdam, Chapter 3 (1985) 125-219.

[5] Blom C E, Altona C, Mol. Phys., 31 (1976) 1377.

[6] Fogarasi G, Spectrochim. Acta Part A, 53 (1997) 1211.

[7] De Mare G R, Panchenko Y N, Bock C W, J. Phys. Chem., 98 (1994), 1416.

[8] Yamakita Y, Tasuni M, J. Phys. Chem. 99 (1995) 8524.

[9] Pongor G, Pulay P, Fogarasi G, Boggs J E, J. Am. Chem. Soc., 106 (1984) 2765.

[10]Jeergal P R, Natti N R, Kannavar M K A, Indian J Pure Appl. Phys., 29 (1991) 752.

[11]Gupta S P, Gupta C, Sharma S, Goel R K, Indian J Pure Appl Phys., 62B (1988) 560.

[12]Martin J M L, Alsenoy C V, J. Phys. Chem. 100 (1996) 6973.

[13]Zhou Zhengyu. Fu Aiping. Du. Nongmei, Int. J. Quant. Chem. 78 (2000) 186.

[14]Krishnakumar V, John Xavier R, Indian Journal of Pure and Applied Physics 41 (2003) 95 – 98.

[15]Singh N P, Yadav R A, Indian Journal of Physics B 75(4) (2001) 347.

[16] Parr R G, Yang W, Density Functional Theory of Atoms and Molecules, Oxford University Press, New York, 1989.
[17]Rauhut G, Pulay P, J. Phys. Chem. 99 (1995) 3093.
[18]Castella - Ventura M, Kassab E, Buntinx G, Poizat O, Phys. Chem. Chem. Phys., 2 (2000) 4682.
[19]Shin D N, Hahn J W, Jung K H, Ha T K, J. Raman Spectrosc., 29 (1998) 245.
[20]Zhengyu Z, Du. Dongmei, Journal of Molecular structure (Theochem.) 505 (2000) 247- 249.
[21]Martin J M L, Alsenoy C V, J. Phys. Chem. 100 (1996) 6973.
[22]Zhou Zhengyu. Fu Aiping. Du. Nongmei, Int. J. Quant. Chem. 78 (2000) 186.
[23]Frisch M J, Trucks G W, Schlegel H B, Scuseria G E, Robb M A, Cheeseman J R, Montgomery J A, Vreven Jr, T, Kudin K N, Burant J C, Millam J M, Iyengar S S, Tomasi J, Barone V, Mennucci B, Cossi M, Scalmani G, Rega N, Petersson G A, Nakatsuji H, Hada M, Ehara M, Toyota K, Fukuda R, Hasegawa J, Ishida M, Nakajima T, Honda Y, Kitao O, Nakai H, Klene M, Li X, Knox J E, Hratchian H P, Cross J B, Adamo C, Jaramillo J, Gomperts R, Stratmann R E, Yazyev O, Austin A J, Cammi R, Pomelli C, Ochterski J W, Ayala P Y, Morokuma K, Voth G A, Ssalvador P, Dannenberg J J, Zakrzewski V G, Dapprich S, Daniels A D, Strain M C, Farkas O, Malick D K, Rabuck A D, Raghavachari K, Foresman J B, Ortiz J V, Cui Q, Baboul A G, Clifford S, Cioslowski J, Stefanov B B, Liu G, Liashenko A, Piskorz P, Komaromi I, Martin R L, Fox D J, Keith T, Al-Laham M A, Peng C Y, Nanayakkara A, Challacombe M, Gill P M W, Johnson B, Chen W, Wong M W, Gonzalez C, and Pople J A, (Gaussian, Inc., Pittsburgh PA, 2009).
[24]Becke A D, J. Chem. Phys., 98 (1993) 5648.
[25]Lee C, Yang W, Parr R G, Phys. Rev., B37 (1988) 785.
[26]Fogarasi G, Zhou X, Taylor P W, Pulay P, J. Am. Chem. Soc., 114(1992)8191- 8201.
[27]Rauhut G, Pulay P, J. Phys. Chem. 99 (1995) 3093.
[28]Sundius T, J. Mol. Struct, 218 (1990) 321 (MOLVIB (V.7.0): Calculation of Hormonic Force Fields and Vibrational Modes of Molecules, QCPE program No.807 (2002).
[29]Polavarapu PL, J. Phys. Chem., 94 (1990) 8106.
[30]Sundius T, Vib. Spectrosc. 29 (2002) 89.
[31]Keresztury G, Holly S, Varga J, Besenyei G, Wang A Y, Durig J R, Spectrochim. Acta Part A, 49 (1993) 2007.
[32]Keresztury G, Raman Spectroscopy: Theory in : J.M. Chalmers, P.R. Griffiths (Ed.), Handbook of Vibrational Spectroscopy, Vol.1, Wiley, 2002.
[33]Fogarasi G, Pulay P, in : J.R. Durig (Ed.), Vibrational Spectra and Structure, Vol.14, Elsevier, Amsterdam, Chapter 3 (1985) 125-219.
[34]Pulay P, in: H.F. Schaefer III (Ed.), Application of Electronic structure Theory, Modern Theoretical Chemistry, Vol.4, Plenum, New York, 197, P.153.
[35]E .Kavitha, N. Sundaraganesan and S.Sebastian, Indian J Pure & Appl. Phys., 48 (2010) 20.
[36]R. John Xavier, V.Balachandran M. Arivazhagan & G. Ilango, Indian J Pure & Appl. Phys., 38 (2010) 245.
[37]N.P.G. Roeges, A Circle to the complete interpretation of infrared spectra of organic structures, Wiley, New York, 1994.
[38]J. Swaminathan, M. Ramalingam, V. Sethuraman, N. Sundaraganesan, S. Sebastian, Spectrochim. Acta. A73 (2009) 593.
[39]G.Ilango, M. Arivazhagan, J.Joseph Prince & V.Balachandran, Indian J Pure & Appl. Phys, 46 (2008) 698.
[40]V. Virendra Kumar, Y. Panikar, M. A. Palafox, J. K. Vats, I.Kostova, K. Lang and V. K. Rastogi, Indian J Pure & Appl. Phys., 48 (2010) 85.
[41]N. B. Colthup, L. H. Daly and S. E. Wiberly, Introduction to Infrared and Raman Spectroscopy (eds. 3, Academic Press, New York), 1990.
[42]C.R. Zhang, H.S. Chen, G.H. Wang, Chem. Res. Chin. U 20 (2004) 640–646.
[43]Y. Sun, X. Chen, L. Sun, X. Guo, W. Lu, Chem. Phys. Lett. 381 (2003) 397–403.
[44]O. Christiansen, J. Gauss, J.F. Stanton, Chem. Phys. Lett. 305 (1999) 147–155.
[45]Z.S. Wang, Y.Y. Huang, C.H. Huang, J. Zheng, H.M. Cheng, S.J. Tian, Synth. Met. 14 (2000) 201–207.
[46]T. Karakurt et al. Journal of Molecular Structure 991 (2011) 186–201.
[47]F.L. Huyskens, P.L. Huyskens, A.P. Person, J. Chem. Phys. 108 (1998) 8161.